

# CP asymmetry from the effect of the isospin symmetry breaking during B-meson decay

Wan-Ying Yao<sup>1\*</sup>, Gang Lü<sup>1†</sup>, Hai-Feng Ou<sup>1‡</sup>

<sup>1</sup> *Institute of Theoretical Physics, College of Science,  
Henan University of Technology, Zhengzhou 450001, China*

The direct CP asymmetry in quasi-two-body decays of  $B \rightarrow (V \rightarrow \pi^+\pi^-)P$  is investigated in the perturbative QCD (PQCD) method, where P represents a pseudoscalar meson and V refers to  $\rho$ ,  $\omega$  and  $\phi$  mesons. We present the amplitude of the quasi-two-body decay process and investigate the effects of mixed resonance involving  $\rho^0 - \omega$ ,  $\rho^0 - \phi$  and  $\omega - \phi$ , while considering the impact of isospin symmetry breaking. We observe a significant CP asymmetry when the invariant mass of the  $\pi^+\pi^-$  pair is within the resonance ranges of  $\rho$ ,  $\omega$  and  $\phi$ . Consequently, we proceed to quantify the regional CP asymmetry in these resonance regions. A significant difference is observed when comparing results obtained with and without interference and isospin conservation. The CP asymmetry results obtained from the three-body decay process, without interference due to isospin conservation by the PQCD method, are in agreement with the newly updated data acquired by the LHCb experiment.

## I. INTRODUCTION

CP asymmetry, which plays a crucial role in elucidating the matter-antimatter asymmetry of the Universe, holds significant theoretical and experimental significance in the field of Particle physics [1, 2]. The breaking of CP symmetry can originate from weak decay of hadron, neutral hadron mixing, or the interference between decay and mixing [3]. In the framework of the Standard Model (SM), CP asymmetry arises due to the presence of a weak complex phase in the Cabibbo-Kobayashi-Maskawa (CKM) matrix, which characterizes the transition from mass eigenstates to weak interaction eigenstates of quarks. CP asymmetry has been experimentally observed in the K, B, and D meson decay process [4–6]. The weak phase difference is determined by the CKM matrix elements, while the strong phase can arise from the hadronic matrix elements and interference among intermediate states. Recently, CP asymmetry has been observed in the course of the B-meson multi-body decay experiment [7, 8]. The investigation of CP asymmetry in multi-body decays of B mesons plays an increasingly pivotal role in both scrutinizing the CKM mechanism of the Standard Model and exploring novel sources of CP asymmetry.

In contrast to the two-body decay, the three-body decay of B meson encompasses both resonance and non-resonance contributions, as well as being influenced by final state re-scattering in  $KK \rightarrow \pi\pi$  interactions [9]. Therefore, it exhibits a greater range of diverse characteristics pertaining to CP asymmetry information, rendering it deserving of attention. The observation of significant CP asymmetry in localized regions of phase space for charmless three-body B-meson decays has been reported through model-independent analyses. In the LHCb experiment, researchers

---

\* Email: 1904132420@qq.com

† Corresponding author Email: ganglv66@sina.com

‡ Email: ouhaifeng@haut.edu.cn

extensively investigated the complete phase space of B meson decay, focusing on a specific invariant mass region. The data used for the integrated CP asymmetries in full phase space,  $A_{CP}^{inte}$ , are obtained from the decay process  $B^\pm \rightarrow \pi^+\pi^-\pi^\pm$ . Similarly, the CP asymmetry values are derived from the decay process of  $B^\pm \rightarrow \pi^+\pi^-\pi^\pm$ , resulting in  $A_{CP}^{low} = 58.4 \pm 8.2 \pm 2.7 \pm 0.7$  and in the rescattering regions with  $1.0 \text{ GeV} < m_{\pi^+\pi^-} < 1.5 \text{ GeV}$ , for the low invariant mass region with  $m_{\pi^+\pi^-}^2_{low} < 0.4 \text{ GeV}^2$  and high invariant mass region with  $m_{\pi^+\pi^-}^2_{high} < 15 \text{ GeV}^2$ , respectively, yielding a value of  $A_{CP}^{resc} = 17.2 \pm 2.1 \pm 1.2 \pm 0.7$  [10, 11]. The data are extracted from the  $B^\pm \rightarrow \pi^+\pi^-K^\pm$  decay for the integrated CP asymmetries in full phase space, where  $A_{CP}^{inte}$  is measured to be  $2.5 \pm 0.4 \pm 0.4 \pm 0.7$ . Additionally, measurements are performed in specific regions: the low invariant mass region ( $0.08 \text{ GeV}^2 < m_{\pi^+\pi^-}^2_{low} < 0.66 \text{ GeV}^2$ ) and the high invariant mass region ( $m_{\pi^\pm K^\pm}^2 < 15 \text{ GeV}^2$ ), yielding  $A_{CP}^{low}$  of  $67.8 \pm 7.8 \pm 3.2 \pm 0.7$  and measurements in rescattering regions with  $1.0 \text{ GeV} < m_{\pi^+\pi^-} < 1.5 \text{ GeV}$  resulting in  $A_{CP}^{resc}$  of  $12.1 \pm 1.2 \pm 1.7 \pm 0.7$  [9, 11].

From the existing experimental data, we can conclude that there is a large CP symmetry in the invariant mass region. Therefore, it has more diverse characteristics in terms of CP symmetry information, which is worthy of academic attention. The decay of three-body B mesons was analyzed by using the Dalitz diagram in the LHCb experiment. The characteristics of the resonance amplitudes can be clearly observed from the diagram, it is found that the scalar and vector resonances with invariant masses less than about  $1\text{GeV}/c^2$  dominate. In the decay of charged B mesons, it is clearly observed from the Dalitz diagram that there are obviously CP symmetry when the invariant masses of  $\pi^+\pi^-$  are in the  $\rho^0(770)$  and  $f^0(980)$  resonance regions. Until recently, a resonance model that accurately describes these effects has been lacking [7, 8]. Although our previous results showed that  $\pi^+\pi^-$  has a large CP symmetry the  $\rho^0(770)$  and  $\omega(782)$  resonance regions [9, 11]. Due to the intermediate state resonance between different isospin mesons and the factor of non-uniformity of phase space distribution is not considered, they cannot be compared with the experimental results.

The charmless decay of B mesons to three hadrons is predominantly governed by a quasi-two-body process involving an intermediate resonance state, and the effects of resonance can be accurately described using the Breit-Wigner (BW) formalism. This decay process encompasses two distinct interference amplitudes between the weak phase and the strong phase. The weak phase is associated with the Cabibbo-Kobayashi-Maskawa (CKM) matrix, while the strong phase arises from rescattering or other mechanisms during the two-body decay process. We aim to investigate the CP asymmetry of vector meson resonance in the three-body decay of B mesons using the perturbative QCD method (pQCD). With a comprehensive exploration of CP asymmetry, various approaches have been employed to describe the multibody decays of B mesons, including QCD factorization (QCDF) [12] and perturbative QCD (pQCD) [13]. The application of various methodologies can induce significant phase differences, thereby exerting an impact on the CP asymmetry observed in the weak decay process of B mesons. The Sudakov factor is incorporated into PQCD to effectively suppress the non-perturbative contribution, while the non-perturbative component is included in the hadronic wave function. The determination of the wave function can be achieved once experimental data are validated. The PQCD method in the decay of B-meson two-body non-leptonic decay has been demonstrated to be consistent with experimental observations for the majority of decay channels. The two-body decay process corresponding to the B meson has indeed been established and further expanded into various three-body decay processes, owing to the adoption of the finite width approximation.

According to the Vector Meson Dominated (VMD) model, the polarization of photons in vacuum leads to the emergence of vector particles such as  $\rho^0$ ,  $\omega$ , and  $\phi$ . The annihilation of  $e^+e^-$  into photons results in the production

of a pair of  $\pi^+\pi^-$  through an intermediate neutral vector meson. The decay of  $\rho^0$  into  $\pi^+\pi^-$  is an isospin-conserving process, while the decays of  $\omega$  and  $\phi$  into pairs of  $\pi^+\pi^-$  involve isospin asymmetry. To better describe these decay processes, we utilize a unitary matrix transformation to convert the ideal field of the intermediate state (non-physical states) into a physical field. By observing interference between the resonant mesons ( $\rho^0$ ,  $\omega$  and  $\phi$ ), valuable insights into their kinetic mechanisms can be obtained. Furthermore, it should be noted that the presence of intermediate resonance hadrons contributes to the formation of a new strong phase, which may have implications for CP asymmetry in hadronic decays. We investigate the impact of mixed resonance of intermediate particles on CP asymmetry in the three-body decay process of B mesons. By examining the decay of vector meson resonances, it will enable more precise measurement of CP asymmetry in future experimental studies. Additionally, this paper also discusses regional variations in CP asymmetry values for comparison with experimental results.

The layout of the present paper is as follows: In Sec. II we discuss resonant contributions to three-body decays of B meson. The quasi-two-body method  $B \rightarrow VP( V \rightarrow PP)$  is employed to investigate the CP asymmetry. In Sec. III is dedicated to the examination of direct CP asymmetry. The regional CP asymmetries arising from the resonance effects of  $\rho^0$ ,  $\omega$ , and  $\phi$  are taken into consideration. We illustrate the form of the three-body decay amplitude of B meson after considering above resonance effect and present the CP asymmetry. The numerical results and discussion on the local CP defect will be presented in Sec. IV. Sec. V contains our conclusions.

## II. EFFECT OF VECTOR MESON RESONANCE ON THREE-BODY DECAY OF B MESONS

### A. mixing mechanism

Based on the Vector Meson Dominated (VMD) model, electrons and positrons annihilate to generate photons, which are further polarized to form vector meson  $\rho^0$ ,  $\omega$ ,  $\phi$ . Then, these vector mesons decay into pairs of  $\pi^+\pi^-$  mesons [15]. In this mechanism, the mixing parameters corresponding to two vector particles can be obtained by using the electromagnetic form factor of the  $\pi$  meson. In the VMD model, vector mesons transfer momentum and the mixed amplitude parameters are correlated with it.

Since the  $\rho_I^0$  ( $\omega_I, \phi_I$ ) resonance state is a non-physical state, we use the unitary matrix R to transform the isospin field into the physical field:  $\rho_I^0$  ( $\omega_I, \phi_I$ )  $\rightarrow$   $\rho^0$  ( $\omega, \phi$ ). The diagonal elements of the unitary matrix R are 1, and the non-diagonal elements represent the information of the  $\rho^0 - \omega - \phi$  mixture. The contribution of high order terms is ignored in the process of this transformation. The resonance effects for  $A_{\rho\omega}$ ,  $B_{\omega\phi}$ , and  $C_{\rho\phi}$  are defined by a set of mixed amplitude parameters, where it holds that  $A_{\rho\omega} = -A_{\omega\rho}$ ,  $B_{\omega\phi} = -B_{\phi\omega}$ , and  $C_{\rho\phi} = -C_{\phi\rho}$ . The amplitude represents a first-order approximation that is dependent on the variable s, which in turn is related to the square of momentum. The expression for R is

$$R = \begin{pmatrix} 1 & -A_{\rho\omega}(s) & -C_{\rho\phi}(s) \\ A_{\rho\omega}(s) & 1 & -B_{\omega\phi}(s) \\ C_{\rho\phi}(s) & B_{\omega\phi}(s) & 1 \end{pmatrix}. \quad (1)$$

According to the transformation relation of the R matrix, the expression form of the resonance state in the physical state is given:  $\phi = C_{\rho\phi}(s)\rho_I^0 + B_{\omega\phi}(s)\omega_I + \phi_I$ ,  $\omega = A_{\rho\omega}(s)\rho_I^0 + \omega_I - B_{\omega\phi}(s)\phi_I$ ,  $\rho^0 = \rho_I^0 - A_{\rho\omega}(s)\omega_I - C_{\rho\phi}(s)\phi_I$ . The relationship between the mixing parameters  $\Pi_{V_i V_j}$  and  $A_{V_i V_j}$  ( $V_i$  and  $V_j$  represent distinct vector mesons) can be deduced from the subsequent equation:

$$A_{\rho\omega} = -A_{\omega\rho} = \frac{\Pi_{\rho\omega}}{(s - m_\rho^2 + im_\rho\Gamma_\rho) - (s - m_\omega^2 + im_\omega\Gamma_\omega)}. \quad (2)$$

$$B_{\omega\phi} = -B_{\phi\omega} = \frac{\Pi_{\omega\phi}}{(s - m_\omega^2 + im_\omega\Gamma_\omega) - (s - m_\phi^2 + im_\phi\Gamma_\phi)}. \quad (3)$$

$$C_{\rho\phi} = -C_{\phi\rho} = \frac{\Pi_{\rho\phi}}{(s - m_\rho^2 + im_\rho\Gamma_\rho) - (s - m_\phi^2 + im_\phi\Gamma_\phi)}. \quad (4)$$

where  $\sqrt{s}$  represents the invariant mass of the  $\pi^+\pi^-$  meson pair,  $m_V$  denotes the mass of the vector meson, and  $\Gamma_V$  signifies the decay width of the vector meson. Considering the mixing mechanism, we define the corresponding parameters as  $\Pi_{V_1 V_2}(s)$ , which are associated with momentum. Our objective is to investigate the impact of this mixing mechanism on CP asymmetry in the  $\omega$  and  $\phi$  resonance regions.

The parameters  $A_{\rho\omega}$ ,  $B_{\omega\phi}$ ,  $C_{\rho\phi}$ , and  $\Pi_{V_i V_j}$  are considered as first-order approximations. Any product of two parameters can be disregarded due to its higher-order nature. We hereby define:

$$\tilde{\Pi}_{\rho\omega} = \frac{(s - m_\rho^2 + im_\rho\Gamma_\rho)\Pi_{\rho\omega}}{(s - m_\rho^2 + im_\rho\Gamma_\rho) - (s - m_\omega^2 + im_\omega\Gamma_\omega)} \quad (5)$$

$$\tilde{\Pi}_{\rho\phi} = \frac{(s - m_\rho^2 + im_\rho\Gamma_\rho)\Pi_{\rho\phi}}{(s - m_\rho^2 + im_\rho\Gamma_\rho) - (s - m_\phi^2 + im_\phi\Gamma_\phi)} \quad (6)$$

$$\tilde{\Pi}_{\omega\phi} = \frac{(s - m_\phi^2 + im_\phi\Gamma_\phi)\Pi_{\omega\phi}}{(s - m_\omega^2 + im_\omega\Gamma_\omega) - (s - m_\phi^2 + im_\phi\Gamma_\phi)} \quad (7)$$

Through the derivation process of the mixed parameters, it can be inferred that a correlation exists between the mixed parameters and  $s$ . These mixed parameters amalgamate the contributions from both resonant and non-resonant components arising due to isospin symmetry breaking effects in the direct decay process, while also exhibiting momentum dependence. Based on the available experimental results, we are able to accurately determine the mixing parameters  $\Pi_{\rho\omega} = -4470 \pm 250 \pm 160 - i(5800 \pm 2000 \pm 1100)\text{MeV}^2$  in the vicinity of the  $\rho$  meson. The mixing parameters  $\Pi_{\phi\rho} = 720 \pm 180 - i(870 \pm 320)\text{MeV}^2$  were obtained near the  $\phi$  meson [16, 17]. Furthermore, a mixing parameter of  $\Pi_{\omega\phi} = 19000 + i(2500 \pm 300)\text{MeV}^2$  was determined in close proximity to the  $\phi$  meson [18].

## B. CP asymmetry induced by interference

The decay  $B \rightarrow (V \rightarrow \pi^+\pi^-)\pi(K)$  is modeled as a quasi-two-body process, where  $V$  represents an intermediate vector meson. The presence of vector meson resonances in the decay process significantly impacts the strong phase, tree, and penguin amplitudes. In Fig.1, for the decay of  $B \rightarrow [\rho^0(\omega, \phi) \rightarrow \pi^+\pi^-]\pi(K)$ , we investigate the impact of various vector meson resonances.

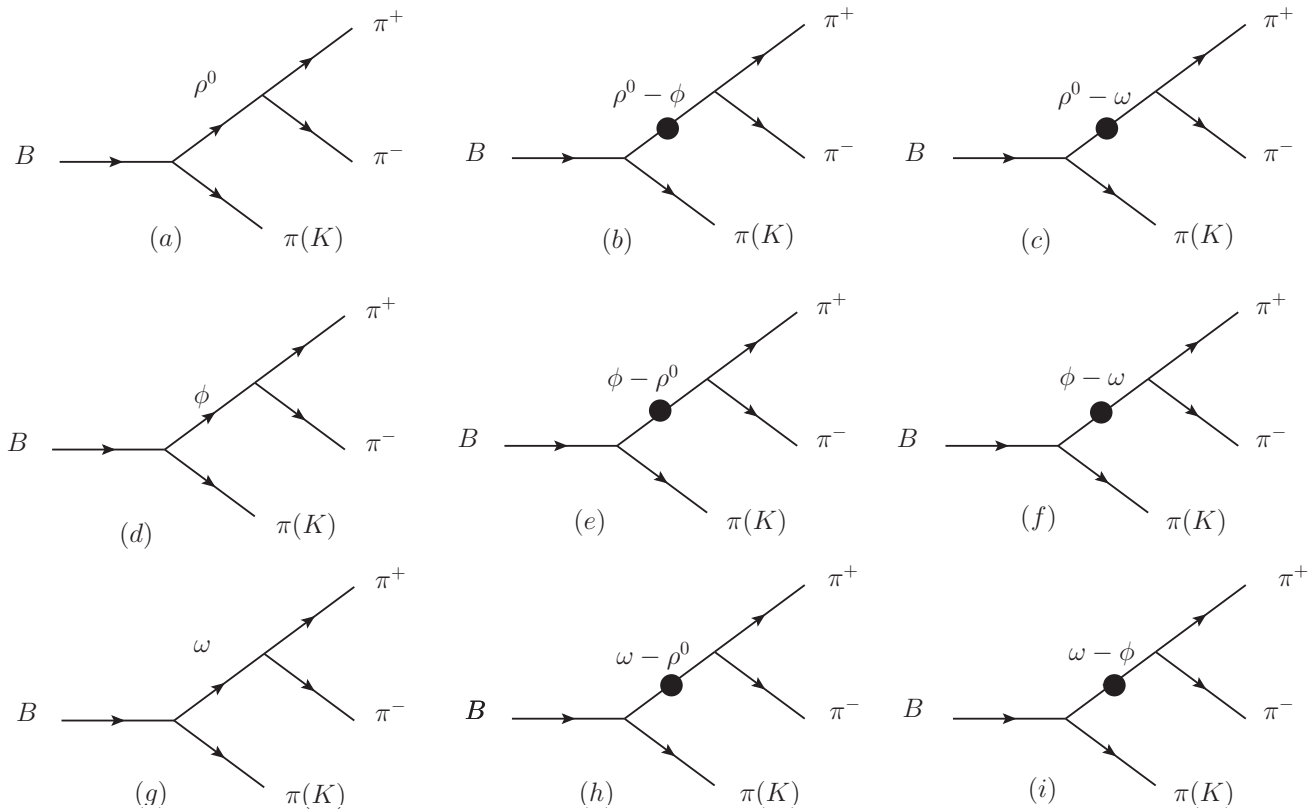


FIG. 1: The diagrams of  $B \rightarrow \pi^+\pi^-\pi(K)$  decay process.

According to the three-vector mixing mechanism and neglecting the contribution of higher order terms, we can derive the decay diagram for the  $B \rightarrow [\rho^0(\omega, \phi) \rightarrow \pi^+\pi^-]\pi(K)$  decay process, as illustrated in Figs (a) ~ (i). In Fig.1(a), it can be observed that the  $\bar{B}_d^0$  undergoes direct decay to produce a pair of  $\pi^+\pi^-$  mesons through the intermediate state of  $\rho^0$ :  $\rho \rightarrow \pi\pi$ . Simultaneously, it is evident that both  $\omega$  ( $\phi$ ) also contribute to the production of pairs of  $\pi^+\pi^-$  mesons via direct decays:  $\phi \rightarrow \pi\pi$  (d), and  $\omega \rightarrow \pi\pi$  (g).

In addition to the direct decay of vector mesons ( $\rho^0$ ,  $\omega$ ,  $\phi$ ) into pairs of  $\pi^+\pi^-$  mesons, the production of such meson pairs can also occur through vector meson resonances (as depicted in figure (b)), including mixed resonances involving  $\rho^0 - \phi$ . During this decay process, isospin symmetry is violated. The black dots in the figure represent these mixing parameters expressed as  $\Pi_{\rho^0\phi}$ . Subsequent figures illustrate various effects arising from mixed resonances and introduce their corresponding mixing parameters.

The decay rate of  $\rho \rightarrow \pi^+\pi^-$  is observed to be 100%, suggesting that the contribution of  $\omega$  and  $\phi$  to the decay of  $\pi^+\pi^-$  can be considered negligible in a rough approximation. However, it is still necessary to take into account

the contribution from this mixing mechanism which produces the strong phases. It should be noted that the mixed parameters  $\Pi_{\rho^0\phi}$ ,  $\Pi_{\rho^0\omega}$ , and  $\Pi_{\omega\phi}$  are approximations at first order. Multiplying any two of these parameters yields a higher-order contribution that can be neglected; hence, cases involving multiple mixed parameters are disregarded.

In conjunction with the significant contributions from the aforementioned diagrams, we present the amplitude expression for the three-body decay process  $B \rightarrow \pi^+\pi^-\pi(K)$ :

$$A = A_T + A_P = \langle \pi^+\pi^-\pi(K)|\mathcal{H}_T|B \rangle + \langle \pi^+\pi^-\pi(K)|\mathcal{H}_P|B \rangle. \quad (8)$$

In the above expression, the matrix element  $\langle \pi^+\pi^-\pi(K)|\mathcal{H}_T|B \rangle$  ( $\langle \pi^+\pi^-\pi(K)|\mathcal{H}_P|B \rangle$ ) contributes to the tree (penguin) graph within an effective Hamiltonian framework. An amplitude analysis of this decay channel reveals that  $\rho^0$  is the dominant contribution. Based on the physical information depicted in the decay diagram, we derive a detailed formulation for both the tree and penguin amplitudes.

$$\begin{aligned} \langle \pi^+\pi^-\pi(K)|H_T|B \rangle &= \frac{g^{\rho^0 \rightarrow \pi^+\pi^-}}{(s - m_{\rho^0}^2 + im_{\rho^0}\Gamma_{\rho^0})(s - m_{\omega}^2 + im_{\omega}\Gamma_{\omega})} \tilde{\Pi}_{\rho\omega} t_{\omega} \\ &+ \frac{g^{\rho^0 \rightarrow \pi^+\pi^-}}{(s - m_{\rho^0}^2 + im_{\rho^0}\Gamma_{\rho^0})(s - m_{\phi}^2 + im_{\phi}\Gamma_{\phi})} \tilde{\Pi}_{\rho^0\phi} t_{\phi} \\ &+ \frac{g^{\rho^0 \rightarrow \pi^+\pi^-}}{s - m_{\rho^0}^2 + im_{\rho^0}\Gamma_{\rho^0}} t_{\rho^0}, \end{aligned} \quad (9)$$

$$\begin{aligned} \langle \pi^+\pi^-\pi(K)|H_P|B \rangle &= \frac{g^{\rho^0 \rightarrow \pi^+\pi^-}}{(s - m_{\rho^0}^2 + im_{\rho^0}\Gamma_{\rho^0})(s - m_{\omega}^2 + im_{\omega}\Gamma_{\omega})} \tilde{\Pi}_{\rho^0\omega} p_{\omega} \\ &+ \frac{g^{\rho^0 \rightarrow \pi^+\pi^-}}{(s - m_{\rho^0}^2 + im_{\rho^0}\Gamma_{\rho^0})(s - m_{\phi}^2 + im_{\phi}\Gamma_{\phi})} \tilde{\Pi}_{\rho^0\phi} p_{\phi} \\ &+ \frac{g^{\rho^0 \rightarrow \pi^+\pi^-}}{s - m_{\rho^0}^2 + im_{\rho^0}\Gamma_{\rho^0}} p_{\rho^0}, \end{aligned} \quad (10)$$

where  $t_V$  and  $p_V$  denote tree contribution and penguin contribution during the decay process  $B \rightarrow V(V = \rho^0, \omega, \phi)\pi(K)$ , respectively.  $g^{\rho^0 \rightarrow \pi^+\pi^-}$  represents the coupling constant of  $\rho \rightarrow \pi\pi$  [19]. We define the differential parameter of CP asymmetry as:

$$A_{CP} = \frac{|A|^2 - |\bar{A}|^2}{|A|^2 + |\bar{A}|^2}. \quad (11)$$

### C. Regional CP asymmetry

Recently, the LHCb team has made a significant discovery indicating the presence of substantial values in a specific region of phase space through direct measurements of CP asymmetry in charmless decays of B mesons involving three-body final states. For instance, the decay process  $B_u^- \rightarrow \pi^+\pi^-\pi^-$  exhibits a significant CP asymmetry within the invariant mass region ( $m_{\pi^+\pi^-}^2 \text{ low} < 0.4 \text{ GeV}^2$ ) [11]. The  $A_{CP}$  integrals are computed in this study to facilitate

the comparison with experimental observations.

The amplitude of the  $B_u^- \rightarrow \rho^0 \pi^-$  decay can be expressed as  $M_{B_u^- \rightarrow \rho^0 \pi^-}^\lambda = \alpha P_{B_u^-} \cdot \epsilon^*(\lambda)$ , where  $\alpha$  represents the effective coupling constant,  $P_{B_u^-}$  denotes the momentum of  $B_u^-$ ,  $\epsilon$  is the polarization vector of  $\rho^0$ , and  $\lambda$  corresponds to the helicity of the vector meson. And the amplitude for  $\rho^0 \rightarrow \pi^+ \pi^-$  can be written as follows:  $M_{\rho^0 \rightarrow \pi^+ \pi^-}^\lambda = g^{\rho^0 \rightarrow \pi^+ \pi^-} \epsilon(\lambda) \cdot (p_\pi^+ - p_\pi^-)$ , where  $g^{\rho^0 \rightarrow \pi^+ \pi^-}$  is the effective coupling constant and  $\epsilon$  refers to the polarization vector of  $\rho^0$ . Hence, the amplitude of  $B_u^- \rightarrow \rho^0 \pi^- \rightarrow \pi^+ \pi^- \pi^-$  is:

$$\begin{aligned}
A &= \frac{g^{\rho^0 \rightarrow \pi^+ \pi^-}}{\alpha} (s - m_{\rho^0}^2 + im_{\rho^0} \Gamma_{\rho^0}) P_{B_u^-}^\mu \sum_{\lambda=\pm 1,0} \epsilon_\mu^*(\lambda) \epsilon_r(\lambda) \cdot (p_\pi^+ - p_\pi^-)^r \\
&= -\frac{g^{\rho^0 \rightarrow \pi^+ \pi^-} \alpha}{(s - m_{\rho^0}^2 + im_{\rho^0} \Gamma_{\rho^0})} P_{B_u^-}^\mu \left[ g_{\mu r} - \frac{(p_\pi^+ + p_\pi^-)_\mu (p_\pi^+ + p_\pi^-)_r}{m_{\rho^0}^2} \right] (p_\pi^+ - p_\pi^-)^r \\
&= \frac{g^{\rho^0 \rightarrow \pi^+ \pi^-}}{(s - m_{\rho^0}^2 + im_{\rho^0} \Gamma_{\rho^0})} \cdot \frac{M_{B_u^- \rightarrow \rho^0 \pi^-}^\lambda}{P_{B_u^-} \cdot \epsilon^*} \cdot (\Sigma - s').
\end{aligned} \tag{12}$$

In the three-body decay process, we employ the principles of momentum and energy conservation to transform the equation:  $P_{B_d^0} = p_\pi^+ + p_\pi^- + p_\pi^0$  and  $m_{i_j}^2 = p_{i_j}^2$ , aiming to facilitate computational procedures. To streamline calculations, we introduce the following definitions:

$$\mathcal{M} = \frac{g^{\rho^0 \rightarrow \pi^+ \pi^-}}{(s - m_{\rho^0}^2 + im_{\rho^0} \Gamma_{\rho^0})} \cdot \frac{M_{B_u^- \rightarrow \rho^0 \pi^-}^\lambda}{P_{B_u^-} \cdot \epsilon^*}. \tag{13}$$

Thus, the amplitude can be written as:

$$A = (\xi - s') \cdot \mathcal{M} \tag{14}$$

where  $\sqrt{s}$  and  $\sqrt{s'}$  represent the low and the high invariant mass of the  $\pi^+ \pi^-$  pair, respectively. Based on the dependency between the values of  $s$ ,  $s'_{\max}$  and  $s'_{\min}$  by setting a fixed value for the variable  $s$ , we can determine an appropriate number  $s'$  that satisfies the formula  $\Sigma = \frac{1}{2}(s'_{\max} + s'_{\min})$ , where  $s'_{\max}$  and  $s'_{\min}$  represent the maximum and minimum values, respectively [20].

According to the kinetic principles of the three-body decay process, we can derive the regional CP violation in the  $B_u^- \rightarrow \pi^+ \pi^- \pi^-$  decay within a certain invariant mass ranges:

$$A_{CP}^\Omega = \frac{\int_{s_1}^{s_2} ds \int_{s_1'}^{s_2'} ds' (\Sigma - s')^2 (|A|^2 - |\bar{A}|^2)}{\int_{s_1}^{s_2} ds \int_{s_1'}^{s_2'} ds' (\Sigma - s')^2 (|A|^2 + |\bar{A}|^2)}. \tag{15}$$

The numerator and denominator of  $A_{CP}$  can be integrated over the range  $\Omega (s_1 < s < s_2, s_1' < s' < s_2')$ . The integration interval for high-invariant mass of  $\pi^+ \pi^-$  meson pairs is  $s_1' < s' < s_2'$ , where  $\int_{s_1'}^{s_2'} ds' (\Sigma - s')^2$  represents a factor dependent on  $s'$ . Through kinematic analysis, the correlation between  $\Sigma$  and  $s'$  can be readily determined. Assuming a finite range, we can consider  $\Sigma$  to be constant. Consequently, the term  $\int_{s_1'}^{s_2'} ds' (\Sigma - s')^2$  becomes negligible in the calculation, rendering  $A_{CP}^\Omega$  independent of the high invariant mass of positive and negative particles.

### III. CALCULATION PROCESS AND ANALYSIS OF CP ASYMMETRY

The narrow width approximation (NWA) is employed in our calculation to decompose the tree body decay process into two successive quasi-two-body decays:  $B \rightarrow (R \rightarrow \pi^+\pi^-)P$ , where R denotes the resonance state and P represents either a  $\pi$  or K meson. Considering the intermediate resonance state R, we introduce the correction factor  $\eta_R$  to define the expression:

$$\eta_R = \frac{\mathcal{B}(B \rightarrow RP_3 \rightarrow P_1P_2P_3)}{\mathcal{B}(B \rightarrow RP_3)\mathcal{B}(B \rightarrow P_1P_2)}, \quad (16)$$

where shows the relationship between the branch ratio measured around the resonance region and the branch ratio of the three-body decay of the B meson [21]. According to the QCD factorization method, the correction factor  $\eta_R$  is about 7% during the decay of  $B_u^- \rightarrow \pi^+\pi^-\pi^-$  [22, 23]. When calculating CP asymmetry, the numerator and denominator terms containing the correction factor  $\eta_R$ . Therefore, we does not consider the width approximation in subsequent calculations.

In calculating CP asymmetry, we consider the contribution of the mixed resonance mechanism to the three-body decay amplitude. The PQCD method is employed in this study to investigate the CP asymmetry effects of vector meson mixing resonance mechanism on B meson decay, encompassing both resonant and non-resonant contributions. The resonant contribution arising from intermediate states is expressed in terms of mixing parameters, while the coupling constants are derived from the decay process of intermediate states into final-state particles. The parameters used in the calculation are derived from Table I .

TABLE I: The decay constants are taken from Refs. Other parameters are from PDG 2022 [24]

Mass(GeV)	$m_{B_u} = 5.27934$	$m_{B_d} = 5.27965$	$m_{\pi^\pm} = 0.140$	$m_{\pi^0} = 0.135$
Wolfenstein parameters	$\lambda = 0.22650$	$A = 0.790$	$\bar{\rho} = 0.141$	$\bar{\eta} = 0.357$
Decay constants (GeV)	$f_{B_s} = 0.23$	$f_B = 0.21$	$f_{\rho(770)} = 0.216$	$f_{\rho(1020)}^T = 0.184$
Decay width (GeV)	$\Gamma_\rho = 0.15$	$\Gamma_\omega = 8.49 \times 10^{-3}$	$\Gamma_\phi = 4.23 \times 10^{-3}$	

#### A. CP asymmetry analysis of the $B_u^- \rightarrow (\rho^0, \omega, \phi \rightarrow \pi^+\pi^-)\pi^-$ decay process

The Dalitz diagram analysis of the decay amplitude  $B^\pm \rightarrow \pi^+\pi^-\pi^\pm$  in two-dimensional phase space is performed, as indicated by relevant research literature. Phenomenological investigations have primarily focused on exploring regional CP asymmetries in the decay process  $B^\pm \rightarrow \pi^+\pi^-\pi^\pm$ , with certain studies emphasizing the significance of  $\rho^0 - \omega$  mixing effects between  $\rho^0$  and  $\omega$ , and highlighting potential interference between the resonance of  $\rho^0$  and the broad S-wave contribution [10, 11]. The resonance contributions of  $\rho - \omega$ ,  $\omega - \phi$ , and  $\rho - \phi$  can give rise to a novel strong phase. To facilitate a clearer observation, we select the energy range of 0.7 GeV to 1.1 GeV, which corresponds to the primary region where the decay processes involving  $\rho^0$ ,  $\omega$ , and  $\phi$  resonances exhibit significant effects.

In experiments, the amplitude analysis of B meson decay in Dalitz plots is commonly used to reconstruct the three-body decay process of B mesons and investigate the momentum relationship in the decay process. However,



due to the fact that the B meson phase space allows for multiple types of resonances to exist, there may be a large number of intermediate states. Investigating these resonance structures is a complex task and it should be noted that it is not possible to distinguish between the contributions made by  $\rho^0$  meson and  $\omega$  meson in experiments. Recently, in the decay process of HCLb to  $B_u^- \rightarrow (\rho^0, \omega, \phi \rightarrow \pi^+ \pi^-) \pi^-$ , clear observations have been made regarding the CP asymmetry effects related to interference between  $\rho^0$  resonance and s-wave. In this work, we initially present the amplitude formulation of the  $B_u^- \rightarrow (\rho^0, \omega, \phi \rightarrow \pi^+ \pi^-) \pi^-$  decay process within the framework of PQCD. By calculating the energy-momentum relationship of the initial meson  $B_u^-$  and final meson  $\pi^+ \pi^-$  decay process using a low-energy effective Hamiltonian, selecting well-established quasi-two-body decay amplitudes, conducting comprehensive analysis on the momentum analysis of the decay process under the coupling constant  $g^{v \rightarrow \pi^+ \pi^-}$ , as well as summing up the polarization vector under the momentum relationship, a new form of amplitude is obtained.

$$\begin{aligned}
\mathcal{A}(B_u^- \rightarrow (\rho^0 \rightarrow \pi^+ \pi^-) \pi^-) &= \frac{\langle \rho^0 K^- | H_{eff} | B_u^- \rangle \langle \pi^+ \pi^- | H_{\rho^0 \rightarrow \pi^+ \pi^-} | \rho^0 \rangle}{s - m_{\rho^0}^2 + i m_{\rho^0} \Gamma_{\rho^0}} \\
&= \sum_{\lambda=0, \pm 1} \frac{G_F P_{(B_u^-)} \cdot \epsilon^*(\lambda) g^{\rho^0 \rightarrow \pi^+ \pi^-} \epsilon(\lambda) \cdot (p_{\pi^+} - p_{\pi^-})}{\sqrt{2}(s - m_{\rho^0}^2 + i m_{\rho^0} \Gamma_{\rho^0})} \\
&\times \left\{ V_{ub} V_{ud}^* \{ a_1 [\mathcal{A}_{ab}^{LL}(\pi, \rho) + \mathcal{A}_{ef}^{LL}(\pi, \rho) - \mathcal{A}_{ef}^{LL}(\rho, \pi)] + a_2 \mathcal{A}_{ab}^{LL}(\rho, \pi) \right. \\
&+ C_2 [\mathcal{A}_{cd}^{LL}(\pi, \rho) + \mathcal{A}_{gh}^{LL}(\pi, \rho) - \mathcal{A}_{gh}^{LL}(\rho, \pi)] + C_1 \mathcal{A}_{cd}^{LL}(\rho, \pi) \} - V_{tb} V_{td}^* \{ (a_4 \\
&+ a_{10}) [\mathcal{A}_{ab}^{LL}(\pi, \rho) + \mathcal{A}_{ef}^{LL}(\pi, \rho) - \mathcal{A}_{ef}^{LL}(\rho, \pi)] + (a_6 + a_8) [\mathcal{A}_{ab}^{SP}(\pi, \rho) \\
&+ \mathcal{A}_{ef}^{SP}(\pi, \rho) - \mathcal{A}_{ef}^{SP}(\rho, \pi)] - (a_4 - \frac{3}{2} a_7 - \frac{3}{2} a_9 - \frac{1}{2} a_{10}) \mathcal{A}_{ab}^{LL}(\rho, \pi) + (C_3 \\
&+ C_9) [\mathcal{A}_{cd}^{LL}(\pi, \rho) + \mathcal{A}_{gh}^{LL}(\pi, \rho) - \mathcal{A}_{gh}^{LL}(\rho, \pi)] + (C_5 + C_7) [\mathcal{A}_{cd}^{SP}(\pi, \rho) \\
&+ \mathcal{A}_{gh}^{SP}(\pi, \rho) - \mathcal{A}_{gh}^{SP}(\rho, \pi)] - (C_3 - \frac{3}{2} C_{10} - \frac{1}{2} C_9) \mathcal{A}_{cd}^{LL}(\rho, \pi) + \frac{3}{2} C_8 \mathcal{A}_{cd}^{LR}(\rho, \pi) \\
&\left. - (C_5 - \frac{1}{2} C_7) \mathcal{A}_{cd}^{SP}(\rho, \pi) \right\}. \tag{17}
\end{aligned}$$

The momentum parameter  $P_i$  ( $P_i = P_{B_u^-}, p_{\pi^+}, p_{\pi^-}$ ) is defined, where  $\epsilon$  represents the polarization vector of the vector meson. The Fermi coupling constant is denoted as  $G_F$ . Three flow structures are labeled as  $LL, LR$ , and  $SP$ .  $\mathcal{A}_{ab}$  refers to factorizable emission diagrams, while  $\mathcal{A}_{cd}$  represents nonfactorizable emission diagrams. Similarly,  $\mathcal{A}_{ef}$  denotes factorizable annihilation diagrams and  $\mathcal{A}_{gh}$  corresponds to nonfactorizable annihilation diagrams.

$$\begin{aligned}
\mathcal{A}(B_u^- \rightarrow (\phi \rightarrow \pi^+ \pi^-) \pi^-) &= \frac{\langle \phi \pi^- | H_{eff} | B_u^- \rangle \langle \pi^+ \pi^- | H_{\phi \rightarrow \pi^+ \pi^-} | \phi \rangle}{s - m_{\phi}^2 + i m_{\phi} \Gamma_{\phi}} \\
&= \sum_{\lambda=0, \pm 1} \frac{G_F P_{B_u^-} \cdot \epsilon^*(\lambda) g^{\phi \rightarrow \pi^+ \pi^-} \epsilon(\lambda) \cdot (p_{\pi^+} - p_{\pi^-})}{\sqrt{2}(s - m_{\phi}^2 + i m_{\phi} \Gamma_{\phi})} \\
&\times \left\{ V_{tb} V_{td}^* \{ (a_3 + a_5 - \frac{1}{2} a_7 - \frac{1}{2} a_9) \mathcal{A}_{ab}^{LL}(\phi, \pi) + (C_4 - \frac{1}{2} C_{10}) \mathcal{A}_{cd}^{LL}(\phi, \pi) \right. \\
&\left. + (C_6 - \frac{1}{2} C_8) \mathcal{A}_{cd}^{LR}(\phi, \pi) \right\}. \tag{18}
\end{aligned}$$

The additional representations of the three-body decay amplitudes that must be taken into account for calculating

CP asymmetry through the mixing mechanism are as follows:  $V_{tb}V_{ts}^* = \lambda$ ,  $V_{ub}V_{us}^* = A\lambda^4(\rho - i\eta)$ ,  $V_{ub}V_{ud}^* = A\lambda^3(\rho - i\eta)(1 - \frac{\lambda^2}{2})$ , and  $V_{tb}V_{td}^* = A\lambda^3(1 - \rho + i\eta)$ .

$$\begin{aligned}
\mathcal{A}(B_u^- \rightarrow (\omega \rightarrow \pi^+\pi^-)\pi^-) &= \frac{\langle \omega\pi^- | H_{eff} | B_u^- \rangle \langle \pi^+\pi^- | H_{\omega \rightarrow \pi^+\pi^-} | \omega \rangle}{s - m_\omega^2 + im_\omega\Gamma_\omega} \\
&= \sum_{\lambda=0,\pm 1} \frac{G_F P_{B_u^-} \cdot \epsilon^*(\lambda) g^{\omega \rightarrow \pi^+\pi^-} \epsilon(\lambda) \cdot (p_{\pi^+} - p_{\pi^-})}{\sqrt{2}(s - m_\omega^2 + im_\omega\Gamma_\omega)} \\
&\times \left\{ V_{ub}V_{ud}^* \{ a_1 [\mathcal{A}_{ab}^{LL}(\pi, \omega) + \mathcal{A}_{ef}^{LL}(\pi, \omega) + \mathcal{A}_{ef}^{LL}(\omega, \pi)] + a_2 \mathcal{A}_{ab}^{LL}(\omega, \pi) \right. \\
&+ C_2 [\mathcal{A}_{cd}^{LL}(\pi, \omega) + \mathcal{A}_{gh}^{LL}(\pi, \omega) + \mathcal{A}_{gh}^{LL}(\omega, \pi)] + C_1 \mathcal{A}_{cd}^{LL}(\omega, \pi) \} \\
&- V_{tb}V_{td}^* \{ (a_4 + a_{10}) [\mathcal{A}_{ab}^{LL}(\pi, \omega) + \mathcal{A}_{ef}^{LL}(\pi, \omega) + \mathcal{A}_{ef}^{LL}(\omega, \pi)] \\
&+ (a_6 + a_8) [\mathcal{A}_{ab}^{SP}(\pi, \omega) + \mathcal{A}_{ef}^{SP}(\pi, \omega) + \mathcal{A}_{ef}^{SP}(\omega, \pi)] \\
&+ (2a_3 + a_4 + 2a_5 + \frac{1}{2}a_7 + \frac{1}{2}a_9 - \frac{1}{2}a_{10}) \mathcal{A}_{ab}^{LL}(\omega, \pi) \\
&+ (C_3 + C_9) [\mathcal{A}_{cd}^{LL}(\pi, \omega) + \mathcal{A}_{gh}^{LL}(\pi, \omega) + \mathcal{A}_{gh}^{LL}(\omega, \pi)] \\
&+ (C_5 + C_7) [\mathcal{A}_{cd}^{SP}(\pi, \omega) + \mathcal{A}_{gh}^{SP}(\pi, \omega) + \mathcal{A}_{gh}^{SP}(\omega, \pi)] \\
&+ (C_3 + 2C_4 - \frac{1}{2}C_9 + \frac{1}{2}C_{10}) \mathcal{A}_{cd}^{LL}(\omega, \pi) \\
&+ (2C_6 + \frac{1}{2}C_8) \mathcal{A}_{cd}^{LR}(\omega, \pi) + (C_5 - \frac{1}{2}C_7) \mathcal{A}_{cd}^{SP}(\omega, \pi) \} \}. \tag{19}
\end{aligned}$$

We present a diagram illustrating the relationship between CP asymmetry and the invariant mass  $\sqrt{s}$  (where  $\sqrt{s}$  represents the invariant mass of  $\pi^+\pi^-$ ) in the quasi-two-body decay  $B_u^- \rightarrow (\rho^0, \omega, \phi \rightarrow \pi^+\pi^-)\pi^-$ , which serves as a theoretical reference for investigating CP asymmetry within the interference range.

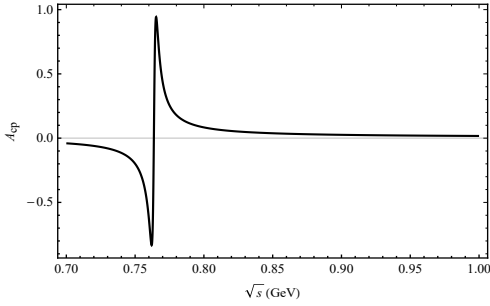


FIG. 2: Plot of  $A_{CP}$  as a function of  $\sqrt{s}$  corresponding to central parameter values of CKM matrix elements for the decay channel of  $B^- \rightarrow \pi^+\pi^-\pi^-$ .

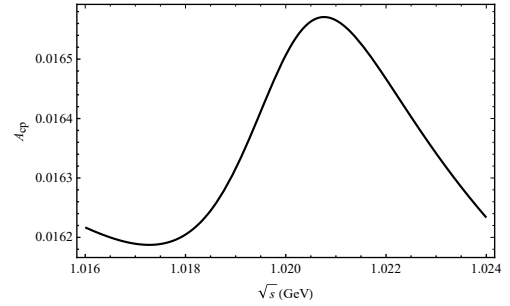


FIG. 3: CP asymmetry plot near the invariant mass of  $\phi$  during the decay channel of  $B^- \rightarrow \pi^+\pi^-\pi^-$  from the central parameter values of CKM matrix elements.

The results for the  $B_u^- \rightarrow \pi^+\pi^-\pi^-$  decay process are presented in Fig.2 and Fig.3. As depicted in Fig.2 and Fig.3, it is evident that the CP violation of the  $B_u^- \rightarrow \pi^+\pi^-\pi^-$  channel undergoes a change when the invariant masses of the  $\pi^+\pi^-$  pair encompass the resonance range of  $\omega$  and  $\phi$ , with a maximum achievable CP asymmetry of 94%. The decay process  $B_u^- \rightarrow \pi^+\pi^-\pi^-$  exhibits a significant variation in CP asymmetry when the invariant masses of the  $\pi^+\pi^-$  pair approaches 0.76 GeV, reaching a peak value of 94%. This behavior can be attributed to the effect arising

from the mixing mechanism between  $\rho^0$  and  $\omega$ . Consequently, interference effects are expected within the range of 0.7 GeV-0.8 GeV as indicated by Fig.2, along with small peaks observed in the invariant mass range corresponding to  $\phi$  according to Fig.3 analysis results. The resulting CP asymmetry is measured at 1.6%, noting that this contribution arises solely from penguin diagram contributions associated with  $B_u^- \rightarrow (\phi \rightarrow \pi^+\pi^-)\pi^-$ .

### B. CP asymmetry analysis of the $B_u^- \rightarrow (\rho^0, \omega, \phi \rightarrow \pi^+\pi^-)K^-$ decay process

The CP asymmetry in the three-body decay of B meson is related to the interference between two-body resonant and three-body non-resonant decays, as well as tree diagram and penguin diagram interference. In experiments, it has been observed that certain local CP asymmetry in phase space are larger than the overall CP asymmetry in phase space. Ever since the perturbative QCD framework for the three-body decay of B meson was proposed, it has been widely applied to various decay processes. perturbative QCD involves calculating the hard part of QCD using perturbation theory, while non-perturbative parts such as interactions between final-state particles are absorbed into hadron wave functions. These hadron wave functions can be determined from experiments and are process-independent, possessing universality. In perturbative QCD, the transverse momentum ( $k_t$ ) is preserved. To address the issue of endpoint divergence, Sudakov factors are introduced to suppress long-range interactions in a small range of transverse momenta, ensuring that the entire process can be calculated perturbatively[25, 26]. This paper adopts the PQCD framework and combines experimental phenomena to study the three-body final state resulting from  $B \rightarrow VP$  meson decay induced by V resonance decay. Considering the resonance effect of vector mesons, namely  $\rho^0$ ,  $\omega$ , and  $\phi$ , we present the decay process  $B_u^- \rightarrow (\rho^0, \omega, \phi \rightarrow \pi^+\pi^-)K^-$  following a similar mechanism.

$$\begin{aligned}
\mathcal{A}(B_u^- \rightarrow (\omega \rightarrow \pi^+\pi^-)K^-) &= \frac{\langle \omega K^- | H_{eff} | B_u^- \rangle \langle \pi^+\pi^- | H_{\omega \rightarrow \pi^+\pi^-} | \omega \rangle}{s - m_\omega^2 + im_\omega \Gamma_\omega} \\
&= \sum_{\lambda=0, \pm 1} \frac{G_F P_{(B_u^-)} \cdot \epsilon^*(\lambda) g^{\omega \rightarrow \pi^+\pi^-} \epsilon(\lambda) \cdot (p_{\pi^+} - p_{\pi^-})}{\sqrt{2}(s - m_\omega^2 + im_\omega \Gamma_\omega)} \\
&\times \left\{ V_{ub} V_{us}^* \{ a_1 [\mathcal{A}_{ab}^{LL}(K, \omega) + \mathcal{A}_{ef}^{LL}(K, \omega)] + a_2 \mathcal{A}_{ab}^{LL}(\omega, K) \right. \\
&+ C_2 [\mathcal{A}_{cd}^{LL}(K, \omega) + \mathcal{A}_{gh}^{LL}(K, \omega)] + C_1 \mathcal{A}_{cd}^{LL}(\omega, K) \} - V_{tb} V_{ts}^* \{ (a_4 \\
&+ a_{10}) [\mathcal{A}_{ab}^{LL}(K, \omega) + \mathcal{A}_{ef}^{LL}(K, \omega)] + (a_6 + a_8) [\mathcal{A}_{ab}^{SP}(K, \omega) \\
&+ \mathcal{A}_{ef}^{SP}(\bar{K}, \omega)] + (2a_3 + 2a_5 + \frac{1}{2}a_7 + \frac{1}{2}a_9) \mathcal{A}_{ab}^{LL}(\omega, K) + (C_3 \\
&+ C_9) [\mathcal{A}_{cd}^{LL}(K, \omega) + \mathcal{A}_{gh}^{LL}(K, \omega)] + (C_5 + C_7) [\mathcal{A}_{cd}^{SP}(K, \omega) + \mathcal{A}_{gh}^{SP}(K, \omega)] \\
&+ (2C_6 + \frac{1}{2}C_8) \mathcal{A}_{cd}^{LR}(\omega, K) + (2C_4 + \frac{1}{2}C_{10}) \mathcal{A}_{cd}^{LL}(\omega, K) \} \}, \tag{20}
\end{aligned}$$

$$\begin{aligned}
\mathcal{A}(B_u^- \rightarrow (\rho^0 \rightarrow \pi^+\pi^-) K^-) &= \frac{\langle \rho^0 K^- | H_{eff} | B_u^- \rangle \langle \pi^+\pi^- | H_{\rho^0 \rightarrow \pi^+\pi^-} | \rho^0 \rangle}{s - m_{\rho^0}^2 + im_{\rho^0} \Gamma_{\rho^0}} \\
&= \sum_{\lambda=0,\pm 1} \frac{G_F P_{(B_u^-)} \cdot \epsilon^*(\lambda) g^{\rho^0 \rightarrow \pi^+\pi^-} \epsilon(\lambda) \cdot (p_{\pi^+} - p_{\pi^-})}{\sqrt{2}(s - m_{\rho^0}^2 + im_{\rho^0} \Gamma_{\rho^0})} \\
&\times \left\{ V_{ub} V_{us}^* \{ a_1 [\mathcal{A}_{ab}^{LL}(K, \rho) + \mathcal{A}_{ef}^{LL}(K, \rho)] + a_2 \mathcal{A}_{ab}^{LL}(\rho, K) + C_2 [\mathcal{A}_{cd}^{LL}(K, \rho) \right. \\
&+ \mathcal{A}_{gh}^{LL}(K, \rho)] + C_1 \mathcal{A}_{cd}^{LL}(\rho, K) \} - V_{tb} V_{ts}^* \{ (a_4 + a_{10}) [\mathcal{A}_{ab}^{LL}(K, \rho) + \mathcal{A}_{ef}^{LL}(K, \rho)] \\
&+ (a_6 + a_8) [\mathcal{A}_{ab}^{SP}(K, \rho) + \mathcal{A}_{ef}^{SP}(K, \rho)] + \frac{3}{2} (a_7 + a_9) \mathcal{A}_{ab}^{LL}(\rho, K) + (C_3 \\
&+ C_9) [\mathcal{A}_{cd}^{LL}(K, \rho) + \mathcal{A}_{gh}^{LL}(K, \rho)] + (C_5 + C_7) [\mathcal{A}_{cd}^{SP}(K, \rho) + \mathcal{A}_{gh}^{SP}(K, \rho)] \\
&+ \frac{3}{2} C_8 \mathcal{A}_{cd}^{LR}(\rho, K) + \frac{3}{2} C_{10} \mathcal{A}_{cd}^{LL}(\rho, K) \} \}, \tag{21}
\end{aligned}$$

$$\begin{aligned}
\mathcal{A}(B_u^- \rightarrow (\phi \rightarrow \pi^+\pi^-) K^-) &= \frac{\langle \phi K^- | H_{eff} | B_u^- \rangle \langle \pi^+\pi^- | H_{\phi \rightarrow \pi^+\pi^-} | \phi \rangle}{s - m_{\phi}^2 + im_{\phi} \Gamma_{\phi}} \\
&= \sum_{\lambda=0,\pm 1} \frac{G_F P_{(B_u^-)} \cdot \epsilon^*(\lambda) g^{\phi \rightarrow \pi^+\pi^-} \epsilon(\lambda) \cdot (p_{\pi^+} - p_{\pi^-})}{\sqrt{2}(s - m_{\phi}^2 + im_{\phi} \Gamma_{\phi})} \\
&\times \left\{ V_{tb} V_{ts}^* \left\{ (a_3 + a_4 + a_5 - \frac{1}{2} a_7 - \frac{1}{2} a_9 - \frac{1}{2} a_{10}) \mathcal{A}_{ab}^{LL}(\phi, K) + (a_4 \right. \\
&+ a_{10}) \mathcal{A}_{ef}^{LL}(\phi, K) + (a_6 + a_8) \mathcal{A}_{ef}^{SP}(\phi, K) (C_3 + C_4 - \frac{1}{2} C_9 \\
&- \frac{1}{2} C_{10}) \mathcal{A}_{cd}^{LL}(\phi, K) + (C_6 - \frac{1}{2} C_8) \mathcal{A}_{cd}^{LR}(\phi, K) + (C_5 - \frac{1}{2} C_7) \\
&\left. \mathcal{A}_{cd}^{SP}(\phi, K) + (C_3 + C_9) \mathcal{A}_{gh}^{LL}(\phi, K) + (C_5 + C_7) \mathcal{A}_{gh}^{SP}(\phi, K) \right\} \}. \tag{22}
\end{aligned}$$

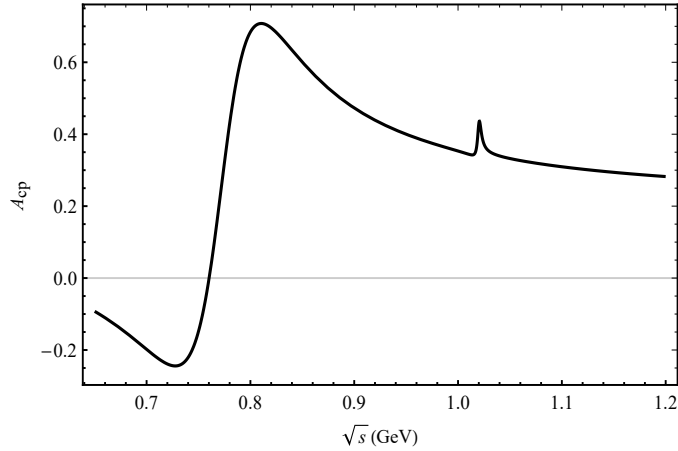


FIG. 4: Plot of  $A_{CP}$  as a function of  $\sqrt{s}$  corresponding to central parameter values of CKM matrix elements for the decay channel of  $B_u^- \rightarrow \pi^+\pi^-K^-$ .

In Fig. 4, the observed behavior of the CP asymmetry in the  $B_u^- \rightarrow \pi^+\pi^-K^-$  decay process provides valuable insights into the dynamics of this decay channel. As we approach the resonance range of  $\omega$ , a significant change in the CP asymmetry is evident, reaching a peak value of 70%. This suggests that there is a strong influence from the

$\omega$  resonance on the decay process.

On the other hand, when we consider the resonance range of  $\phi$ , only slight variations in CP asymmetry are observed. This can be attributed to several factors. It should be noted that for the specific decay process  $B_u^- \rightarrow (\phi \rightarrow \pi^+\pi^-)K^-$ , which involves penguin diagram contribution exclusively, its overall amplitude is further diminished due to interference from  $\phi - \rho$  mixing resonance. This interference effect leads to a reduction in observable changes in CP asymmetry near the resonance range of  $\phi$ .

### C. CP asymmetry analysis of the $\bar{B}_d^0 \rightarrow (\rho^0, \omega, \phi \rightarrow \pi^+\pi^-)\pi^0$ decay process

Considering the vector meson  $\rho^0 - \omega - \phi$  resonance effect, the process of  $\bar{B}_d^0 \rightarrow \pi^+\pi^-\pi^0$  can be further elaborated. The presence of these vector mesons in the decay channel introduces additional dynamics and interactions that contribute to the overall behavior of this process. They play a crucial role in understanding strong interactions. In particular, their resonant behavior is associated with a peak in the CP asymmetry for certain energy ranges.

In the decay process of  $\bar{B}_d^0 \rightarrow \pi^+\pi^-\pi^0$ , the vector meson resonance effect refers to how these particles can influence or modify the decay process. By considering this resonance effect, we gain insights into various aspects of  $\bar{B}_d^0 \rightarrow \pi^+\pi^-\pi^0$ . For instance, it helps us understand how different intermediate states involving vector mesons contribute to the final state particles (pions) observed experimentally. It also provides information about possible interference patterns between different amplitudes contributing to this decay process. The amplitudes of the decay process  $\bar{B}_d^0 \rightarrow \pi^+\pi^-\pi^0$  from the different intermediate vector meson can be expressed as

$$\begin{aligned}
\mathcal{A}(\bar{B}_d^0 \rightarrow (\rho^0 \rightarrow \pi^+\pi^-)\pi^0) &= \frac{\langle \rho^0 \pi^0 | H_{eff} | \bar{B}^0 \rangle \langle \pi^+\pi^- | H_{\rho^0 \rightarrow \pi^+\pi^-} | \rho^0 \rangle}{s - m_{\rho^0}^2 + im_{\rho^0} \Gamma_{\rho^0}} \\
&= \sum_{\lambda=0, \pm 1} \frac{G_F P_{\bar{B}^0} \cdot \epsilon^*(\lambda) g^{\rho^0 \rightarrow \pi^+\pi^-} \epsilon(\lambda) \cdot (p_{\pi^+} - p_{\pi^-})}{\sqrt{2}(s - m_{\rho^0}^2 + im_{\rho^0} \Gamma_{\rho^0})} \\
&\times \{ V_{ub} V_{ud}^* \{ a_2 [ -\mathcal{A}_{ab}^{LL}(\pi, \rho) - \mathcal{A}_{ab}^{LL}(\rho, \pi) + \mathcal{A}_{ef}^{LL}(\pi, \rho) + \mathcal{A}_{ef}^{LL}(\rho, \pi) ] \\
&+ C_1 [ -\mathcal{A}_{cd}^{LL}(\pi, \rho) - \mathcal{A}_{cd}^{LL}(\rho, \pi) + \mathcal{A}_{gh}^{LL}(\pi, \rho) + \mathcal{A}_{gh}^{LL}(\rho, \pi) ] \} \\
&- V_{tb} V_{td}^* \{ (a_4 - \frac{3}{2} a_9 - \frac{1}{2} a_{10}) [ \mathcal{A}_{ab}^{LL}(\pi, \rho) + \mathcal{A}_{ab}^{LL}(\rho, \pi) ] + \frac{3}{2} a_7 [ \mathcal{A}_{ab}^{LL}(\pi, \rho) \\
&- \mathcal{A}_{ab}^{LL}(\rho, \pi) ] + (C_3 - \frac{1}{2} C_9 - \frac{3}{2} C_{10}) [ \mathcal{A}_{cd}^{LL}(\pi, \rho) + \mathcal{A}_{cd}^{LL}(\rho, \pi) ] \\
&- \frac{3}{2} C_8 [ \mathcal{A}_{cd}^{LR}(\pi, \rho) + \mathcal{A}_{cd}^{LR}(\rho, \pi) ] + (a_6 - \frac{1}{2} a_8) [ \mathcal{A}_{ab}^{SP}(\pi, \rho) + \mathcal{A}_{ef}^{SP}(\pi, \rho) \\
&+ \mathcal{A}_{ef}^{SP}(\rho, \pi) ] + (C_5 - \frac{1}{2} C_7) [ \mathcal{A}_{cd}^{SP}(\pi, \rho) + \mathcal{A}_{cd}^{SP}(\rho, \pi) + \mathcal{A}_{gh}^{SP}(\pi, \rho) \\
&+ (2 a_3 + a_4 - 2 a_5 - \frac{1}{2} a_7 + \frac{1}{2} a_9 - \frac{1}{2} a_{10}) [ \mathcal{A}_{ef}^{LL}(\pi, \rho) + \mathcal{A}_{ef}^{LL}(\rho, \pi) ] \\
&+ (C_3 + 2 C_4 - \frac{1}{2} C_9 + \frac{1}{2} C_{10}) [ \mathcal{A}_{gh}^{LL}(\pi, \rho) + \mathcal{A}_{gh}^{LL}(\rho, \pi) ] \\
&+ (2 C_6 + \frac{1}{2} C_8) [ \mathcal{A}_{gh}^{LR}(\pi, \rho) + \mathcal{A}_{gh}^{LR}(\rho, \pi) ] \} \}, \tag{23}
\end{aligned}$$

$$\begin{aligned}
\mathcal{A}(\bar{B}_d^0 \rightarrow (\omega \rightarrow \pi^+\pi^-)\pi^0) &= \frac{\langle \omega \pi^0 | H_{eff} | \bar{B}^0 \rangle \langle \pi^+\pi^- | H_{\omega \rightarrow \pi^+\pi^-} | \omega \rangle}{s - m_\omega^2 + im_\omega \Gamma_\omega} \\
&= \sum_{\lambda=0,\pm 1} \frac{G_F P_{(\bar{B}^0)} \cdot \epsilon^*(\lambda) g^{\omega \rightarrow \pi^+\pi^-} \epsilon(\lambda) \cdot (p_{\pi^+} - p_{\pi^-})}{\sqrt{2}(s - m_\omega^2 + im_\omega \Gamma_\omega)} \\
&\quad \times \{ V_{ub} V_{ud}^* \{ a_2 [\mathcal{A}_{ab}^{LL}(\pi, \omega) - \mathcal{A}_{ab}^{LL}(\omega, \pi) + \mathcal{A}_{ef}^{LL}(\pi, \omega) + \mathcal{A}_{ef}^{LL}(\omega, \pi)] \\
&\quad + C_1 [\mathcal{A}_{cd}^{LL}(\pi, \omega) - \mathcal{A}_{cd}^{LL}(\omega, \pi) + \mathcal{A}_{gh}^{LL}(\pi, \omega) + \mathcal{A}_{gh}^{LL}(\omega, \pi)] \} \\
&\quad - V_{tb} V_{td}^* \{ - (2a_3 + a_4 + 2a_5 + \frac{1}{2}a_7 + \frac{1}{2}a_9 - \frac{1}{2}a_{10}) \mathcal{A}_{ab}^{LL}(\omega, \pi) \\
&\quad - (C_3 + 2C_4 - \frac{1}{2}C_9 + \frac{1}{2}C_{10}) \mathcal{A}_{cd}^{LL}(\omega, \pi) - (2C_6 + \frac{1}{2}C_8) \mathcal{A}_{cd}^{LR}(\omega, \pi) \\
&\quad - (a_4 + \frac{3}{2}a_7 - \frac{3}{2}a_9 - \frac{1}{2}a_{10}) [\mathcal{A}_{ab}^{LL}(\pi, \omega) + \mathcal{A}_{ef}^{LL}(\pi, \omega) + \mathcal{A}_{ef}^{LL}(\omega, \pi)] \\
&\quad - (C_3 - \frac{1}{2}C_9 - \frac{3}{2}C_{10}) [\mathcal{A}_{cd}^{LL}(\pi, \omega) + \mathcal{A}_{gh}^{LL}(\pi, \omega) + \mathcal{A}_{gh}^{LL}(\omega, \pi)] \\
&\quad + \frac{3}{2}C_8 [\mathcal{A}_{cd}^{LR}(\pi, \omega) + \mathcal{A}_{gh}^{LR}(\pi, \omega) + \mathcal{A}_{gh}^{LR}(\omega, \pi)] \\
&\quad - (a_6 - \frac{1}{2}a_8) [\mathcal{A}_{ab}^{SP}(\pi, \omega) + \mathcal{A}_{ef}^{SP}(\pi, \omega) + \mathcal{A}_{ef}^{SP}(\omega, \pi)] \\
&\quad - (C_5 - \frac{1}{2}C_7) [\mathcal{A}_{cd}^{SP}(\pi, \omega) + \mathcal{A}_{cd}^{SP}(\omega, \pi) + \mathcal{A}_{gh}^{SP}(\pi, \omega) + \mathcal{A}_{gh}^{SP}(\omega, \pi)] \} \}, \tag{24}
\end{aligned}$$

$$\begin{aligned}
\mathcal{A}(\bar{B}_d^0 \rightarrow (\phi \rightarrow \pi^+\pi^-)\pi^0) &= \frac{\langle \phi \pi^0 | H_{eff} | \bar{B}^0 \rangle \langle \pi^+\pi^- | H_{\phi \rightarrow \pi^+\pi^-} | \phi \rangle}{s - m_\phi^2 + im_\phi \Gamma_\phi} \\
&= \sum_{\lambda=0,\pm 1} \frac{G_F P_{(\bar{B}^0)} \cdot \epsilon^*(\lambda) g^{\phi \rightarrow \pi^+\pi^-} \epsilon(\lambda) \cdot (p_{\pi^+} - p_{\pi^-})}{\sqrt{2}(s - m_\phi^2 + im_\phi \Gamma_\phi)} \\
&\quad \times \{ V_{tb} V_{td}^* \{ (a_3 + a_5 - \frac{1}{2}a_7 - \frac{1}{2}a_9) \mathcal{A}_{ab}^{LL}(\phi, \pi) + (C_4 - \frac{1}{2}C_{10}) \mathcal{A}_{cd}^{LL}(\phi, \pi) \\
&\quad + (C_6 - \frac{1}{2}C_8) \mathcal{A}_{cd}^{LR}(\phi, \pi) \} \}. \tag{25}
\end{aligned}$$

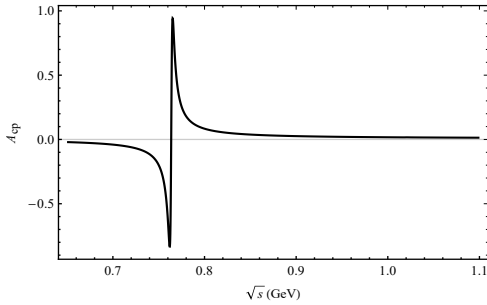


FIG. 5: Plot of  $A_{CP}$  as a function of  $\sqrt{s}$  corresponding to central parameter values of CKM matrix elements for the decay channel of  $\bar{B}_d^0 \rightarrow \pi^+\pi^-\pi^0$ .

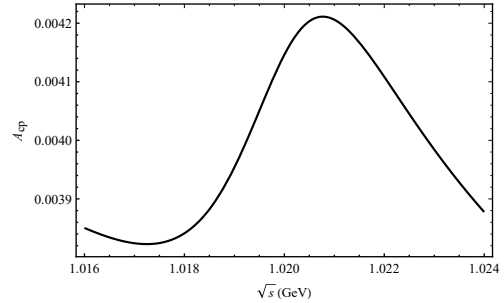


FIG. 6: CP asymmetry plot near the invariant mass of  $\phi$  during the decay channel of  $B_d^0 \rightarrow \pi^+\pi^-\pi^0$  from the central parameter values of CKM matrix elements.

In Fig.5, we present the relationship between the invariant mass of the  $\pi^+\pi^-$  meson pair and the CP asymmetry

in the decay process  $\bar{B}_d^0 \rightarrow \pi^+\pi^-\pi^0$ . We aim to investigate how changes in the meson pair invariant mass affect CP asymmetry.

Within a specific range of invariant masses, we observe a significant variation in CP asymmetry within the  $\rho^0$ - $\omega$ - $\phi$  mass region. The maximum value of CP asymmetry reaches an impressive 91%. Notably, slight peaks are observed at positions corresponding to the mass of the  $\phi$  meson.

To gain further insights into these observations, we investigate the impact of both three-particle and two-particle mixing effects on CP asymmetry in this decay process. By conducting regional integration analysis of CP and examining resonance effects on CP asymmetry, we enhance our understanding of the contributions from different factors to variations in CP violation. Detailed discussions regarding this topic are presented in the subsequent section.

Additionally, it is worth mentioning that another related decay process involving penguins diagrams is investigated:  $\bar{B}_d^0 \rightarrow (\phi \rightarrow \pi^+\pi^-)\pi^0$ . Unlike our previous discussion on tree contributions, this particular decay process solely relies on penguins diagrams without any involvement from tree contributions.

#### D. CP asymmetry analysis of the $\bar{B}_d^0 \rightarrow (\rho^0, \omega, \phi \rightarrow \pi^+\pi^-)\bar{K}^0$ decay process

In the above amplitude analysis, we investigated the impact of vector meson resonance effects on decay processes. During the decay process, vector meson resonances can induce the generation of strong phases. In CP asymmetry diagrams, different vector meson resonances can be observed to have varying effects on the CP asymmetry of decay processes. Currently, there is no experimental data available on the  $\bar{B}_d^0 \rightarrow (\rho^0, \omega, \phi \rightarrow \pi^+\pi^-)\bar{K}^0$  decay process. Studying the vector meson resonance effect not only provides rich physical information to explore the energy-momentum relationship in multi-body decay processes, but also offers a new approach for future experimental investigations of CP asymmetry values and intermediate mesons in  $\bar{B}_d^0 \rightarrow (\rho^0, \omega, \phi \rightarrow \pi^+\pi^-)\bar{K}^0$  decay processes. We present the amplitude form of the  $\bar{B}_d^0 \rightarrow (\rho^0, \omega, \phi \rightarrow \pi^+\pi^-)\bar{K}^0$  decay process under the PQCD framework.

$$\begin{aligned}
\mathcal{A}(\bar{B}_d^0 \rightarrow (\omega \rightarrow \pi^+\pi^-)\bar{K}^0) &= \frac{\langle \omega \bar{K}^0 | H_{eff} | \bar{B}_d^0 \rangle \langle \pi^+\pi^- | H_{\omega \rightarrow \pi^+\pi^-} | \omega \rangle}{s - m_\omega^2 + im_\omega \Gamma_\omega} \\
&= \sum_{\lambda=0, \pm 1} \frac{G_F P_{\bar{B}^0} \cdot \epsilon^*(\lambda) g^{\omega \rightarrow \pi^+\pi^-} \epsilon(\lambda) \cdot (p_{\pi^+} - p_{\pi^-})}{2(s - m_\omega^2 + im_\omega \Gamma_\omega)} \\
&\quad \times \{V_{ub} V_{us}^* \{a_2 [\mathcal{A}_{ab}^{LL}(\omega, \bar{K})] + C_1 [\mathcal{A}_{cd}^{LL}(\omega, \bar{K})]\} \\
&\quad \times \{V_{tb} V_{ts}^* \{(a_4 - \frac{1}{2} a_{10}) [\mathcal{A}_{ab}^{LL}(\bar{K}, \omega) + \mathcal{A}_{ef}^{LL}(\bar{K}, \omega)] + (C_3 \\
&\quad - \frac{1}{2} C_9) [\mathcal{A}_{cd}^{LL}(\bar{K}, \omega) + \mathcal{A}_{gh}^{LL}(\bar{K}, \omega)] + (a_6 - \frac{1}{2} a_8) [\mathcal{A}_{ab}^{SP}(\bar{K}, \omega) \\
&\quad + \mathcal{A}_{ef}^{SP}(\bar{K}, \omega)] + (C_5 - \frac{1}{2} C_7) [\mathcal{A}_{cd}^{SP}(\bar{K}, \omega) + \mathcal{A}_{gh}^{SP}(\bar{K}, \omega)] \\
&\quad + (2a_3 + 2a_5 + \frac{1}{2} a_7 + \frac{1}{2} a_9) \mathcal{A}_{ab}^{LL}(\omega, \bar{K}) + (2C_4 \\
&\quad + \frac{1}{2} C_{10}) \mathcal{A}_{cd}^{LL}(\omega, \bar{K}) + (2C_6 + \frac{1}{2} C_8) \mathcal{A}_{cd}^{LR}(\omega, \bar{K})\}\},
\end{aligned} \tag{26}$$

$$\begin{aligned}
\mathcal{A}(\bar{B}_d^0 \rightarrow (\rho^0 \rightarrow \pi^+ \pi^-) \bar{K}^0) &= \frac{\langle \rho^0 \bar{K}^0 | H_{eff} | \bar{B}^0 \rangle \langle \pi^+ \pi^- | H_{\rho^0 \rightarrow \pi^+ \pi^-} | \rho^0 \rangle}{s - m_{\rho^0}^2 + im_{\rho^0} \Gamma_{\rho^0}} \\
&= \sum_{\lambda=0, \pm 1} \frac{G_F P_{\bar{B}^0} \cdot \epsilon^*(\lambda) g^{\rho^0 \rightarrow \pi^+ \pi^-} \epsilon(\lambda) \cdot (p_{\pi^+} - p_{\pi^-})}{2(s - m_{\rho^0}^2 + im_{\rho^0} \Gamma_{\rho^0})} \\
&\quad \times \{V_{ub} V_{us}^* \{a_2 [\mathcal{A}_{ab}^{LL}(\rho, \bar{K})] + C_1 [\mathcal{A}_{cd}^{LL}(\rho, \bar{K})]\} \times \{V_{tb} V_{ts}^* \\
&\quad \{(a_4 - \frac{1}{2} a_{10}) [\mathcal{A}_{ab}^{LL}(\bar{K}, \rho) + \mathcal{A}_{ef}^{LL}(\bar{K}, \rho)] + (C_3 - \frac{1}{2} C_9) [\mathcal{A}_{cd}^{LL}(\bar{K}, \rho) \\
&\quad + \mathcal{A}_{gh}^{LL}(\bar{K}, \rho)] + (a_6 - \frac{1}{2} a_8) [\mathcal{A}_{ab}^{SP}(\bar{K}, \rho) + \mathcal{A}_{ef}^{SP}(\bar{K}, \rho)] + (C_5 - \\
&\quad \frac{1}{2} C_7) [\mathcal{A}_{cd}^{SP}(\bar{K}, \rho) + \mathcal{A}_{gh}^{SP}(\bar{K}, \rho)] - \frac{3}{2} (a_7 + a_9) \mathcal{A}_{ab}^{LL}(\rho, \bar{K}) \\
&\quad - \frac{3}{2} C_8 \mathcal{A}_{cd}^{LR}(\rho, \bar{K}) - \frac{3}{2} C_{10} \mathcal{A}_{cd}^{LL}(\rho, \bar{K})\}\},
\end{aligned} \tag{27}$$

$$\begin{aligned}
\mathcal{A}(\bar{B}_d^0 \rightarrow (\phi \rightarrow \pi^+ \pi^-) \bar{K}^0) &= \frac{\langle \phi \bar{K}^0 | H_{eff} | \bar{B}^0 \rangle \langle \pi^+ \pi^- | H_{\phi \rightarrow \pi^+ \pi^-} | \phi \rangle}{s - m_{\phi}^2 + im_{\phi} \Gamma_{\phi}} \\
&= \sum_{\lambda=0, \pm 1} \frac{G_F P_{\bar{B}^0} \cdot \epsilon^*(\lambda) g^{\phi \rightarrow \pi^+ \pi^-} \epsilon(\lambda) \cdot (p_{\pi^+} - p_{\pi^-})}{\sqrt{2}(s - m_{\phi}^2 + im_{\phi} \Gamma_{\phi})} \\
&\quad \times \{V_{tb} V_{ts}^* \{(a_3 + a_4 + a_5 - \frac{1}{2} a_7 - \frac{1}{2} a_9 - \frac{1}{2} a_{10}) \mathcal{A}_{ab}^{LL}(\phi, \bar{K}) \\
&\quad + (a_4 - \frac{1}{2} a_{10}) \mathcal{A}_{ef}^{LL}(\phi, \bar{K}) + (a_6 - \frac{1}{2} a_8) \mathcal{A}_{ef}^{SP}(\phi, \bar{K}) \\
&\quad + (C_3 + C_4 - \frac{1}{2} C_9 - \frac{1}{2} C_{10}) \mathcal{A}_{cd}^{LL}(\phi, \bar{K}) + (C_6 - \frac{1}{2} C_8) \mathcal{A}_{cd}^{LR}(\phi, \bar{K}) \\
&\quad + (C_5 - \frac{1}{2} C_7) [\mathcal{A}_{cd}^{SP}(\phi, \bar{K}) + \mathcal{A}_{gh}^{SP}(\phi, \bar{K})] + (C_3 - \frac{1}{2} C_9) \mathcal{A}_{gh}^{LL}(\phi, \bar{K})\}\},
\end{aligned} \tag{28}$$

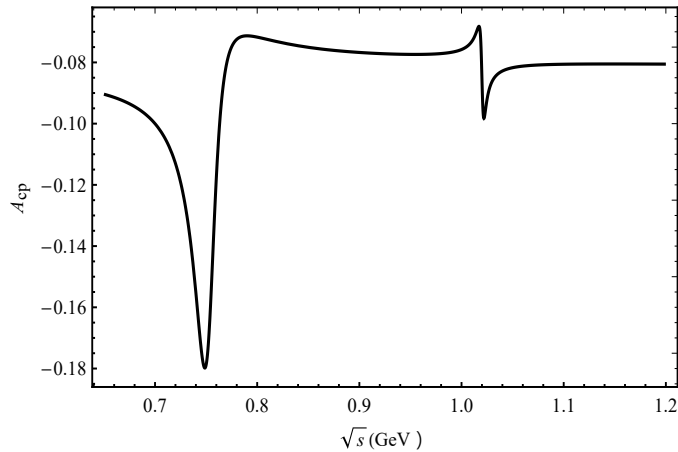


FIG. 7: Plot of  $A_{CP}$  as a function of  $\sqrt{s}$  corresponding to central parameter values of CKM matrix elements for the decay channel of  $\bar{B}_d^0 \rightarrow \pi^+ \pi^- \bar{K}^0$ .

The results for the  $\bar{B}_d^0 \rightarrow \pi^+ \pi^- \bar{K}^0$  decay process are presented in Fig. 6. As depicted in Fig. 6, it is evident that the CP asymmetry of the  $\bar{B}_d^0 \rightarrow \pi^+ \pi^- \bar{K}^0$  channel undergoes variations when the invariant masses of the  $\pi^+ \pi^-$  pair



encompass the ranges corresponding to resonances such as  $\omega$  and  $\phi$ . Notably, a maximum CP asymmetry of 18% can be achieved.

The CP asymmetry in the decay process  $\bar{B}_d^0 \rightarrow \pi^+\pi^-\bar{K}^0$  exhibits a significant change when the invariant mass of the  $\pi^+\pi^-$  pair approaches 0.75 GeV, reaching a peak value of 18%. This behavior can be attributed to the interference effect arising from the  $\rho - \omega$  mixing mechanism, which is expected to occur within the range of 0.7 GeV - 0.8 GeV. Additionally, small peaks are observed in the invariant mass range corresponding to  $\phi$ . The CP asymmetry in this case amounts to 9%. In  $B_d^0 \rightarrow (\phi \rightarrow \pi^+\pi^-)\bar{K}^0$  decay, penguin graph contributions play a role. Notably, the resonance effect due to  $\rho - \phi$  mixing significantly influences CP violation with an associated CP asymmetry value of 9%.

#### IV. ANALYSIS OF REGIONAL CP ASYMMETRY IN THE DECAY PROCESS

TABLE II: The peak regional ( $0.70\text{GeV} \leq \sqrt{s} \leq 1.10\text{GeV}$ ) integral of  $A_{\text{CP}}^{\Omega}$  from different resonance rangs for  $\bar{B}_d \rightarrow \pi^+\pi^-K^0$ ,  $\bar{B}_d \rightarrow \pi^+\pi^-\pi^0$  and  $B_u^- \rightarrow \pi^+\pi^-K^-$ ,  $B_u^- \rightarrow \pi^+\pi^-\pi^-$  decay processes.

Decay channel	This work	Previous measurements(no mixing)
$\bar{B}_d \rightarrow \pi^+\pi^-\bar{K}^0$	$-0.1683 \pm 0.0013 \pm 0.0000$ ( $\rho$ )	
	$-0.0847 \pm 0.0000 \pm 0.0084$ ( $\rho - \omega$ mixing )	—————
	$-0.0813 \pm 0.0064 \pm 0.0052$ ( $\rho - \phi$ mixing)	
	$-0.0847 \pm 0.0056 \pm 0.0089$ ( $\phi - \rho - \omega$ mixing )	
$\bar{B}_d \rightarrow \pi^+\pi^-\pi^0$	$-0.0054 \pm 0.0004 \pm 0.0011$ ( $\rho$ )	
	$0.0173 \pm 0.0109 \pm 0.0015$ ( $\rho - \omega$ mixing )	—————
	$-0.0055 \pm 0.0006 \pm 0.0011$ ( $\rho - \phi$ mixing )	
	$0.0147 \pm 0.0014 \pm 0.0086$ ( $\phi - \rho - \omega$ mixing)	
$B_u^- \rightarrow \pi^+\pi^-K^-$	$0.2093 \pm 0.0206 \pm 0.0044$ ( $\rho$ )	$0.150 \pm 0.019 \pm 0.011$ LHCb[8]
	$0.1771 \pm 0.0084 \pm 0.0061$ ( $\rho - \omega$ mixing )	$0.44 \pm 0.10 \pm 0.04$ BaBar[28]
	$0.2109 \pm 0.0207 \pm 0.0023$ ( $\rho - \phi$ mixing)	$0.30 \pm 0.11 \pm 0.02$ Belle[29]
	$0.3470 \pm 0.0310 \pm 0.0709$ ( $\phi - \rho - \omega$ mixing)	
$B_u^- \rightarrow \pi^+\pi^-\pi^-$	$0.0065 \pm 0.0014 \pm 0.0031$ ( $\rho$ )	$-0.004 \pm 0.017 \pm 0.009$ LHCb[8]
	$0.0256 \pm 0.0013 \pm 0.0016$ ( $\rho - \omega$ mixing)	$0.30 \pm 0.11 \pm 0.02$ Belle[29]
	$0.0076 \pm 0.0006 \pm 0.0023$ ( $\rho - \phi$ mixing)	
	$0.0260 \pm 0.0034 \pm 0.0047$ ( $\phi - \rho - \omega$ mixing)	

In Table 2, we present a comparison between our calculated results and the existing experimental data. Notably,

intriguing observations of significant regional CP asymmetry have been reported in experiments conducted by LHCb, BaBar, and Belle collaborations. Subsequently, we investigate the influence of different resonance effects on regional CP asymmetry. Due to the close masses of  $\rho$  and  $\omega$  mesons in these experiments, distinguishing between them becomes challenging. To address this issue, we incorporate this scenario into our calculations using the PQCD method within the resonance framework for decay channels such as  $\bar{B}_d \rightarrow \pi^+\pi^-\bar{K}^0$ ,  $\bar{B}_d \rightarrow \pi^+\pi^-\pi^0$ ,  $B_u^- \rightarrow \pi^+\pi^-K^-$  and  $B_u^- \rightarrow \pi^+\pi^-\pi^-$ . Our results align with experimental error ranges, validating the accuracy of our calculation method. Specifically in the decay channel of  $\bar{B}_d \rightarrow \pi^+\pi^-\bar{K}^0$ , we observe that resonance contributions from three-particle mixtures significantly impact CP asymmetry.

For vector particle resonances, the decay processes  $\bar{B}_d \rightarrow \pi^+\pi^-\pi^0$  and  $B_u^- \rightarrow \pi^+\pi^-\pi^-$  exhibit significant contributions to CP asymmetry compared to non-resonant decays. It is noteworthy that clear manifestations of CP asymmetry are observed within the resonance range. In the decay channel of  $B_u^- \rightarrow \pi^+\pi^-K^-$ , resonance effects contribute more prominently to CP asymmetry, resulting in increased regional values similar to those observed in the decay channel  $\bar{B}_d \rightarrow \pi^+\pi^-K^0$  within their respective invariant mass ranges.

The calculation of the  $1/m_b$  power correction by perturbation theory is uncertain. Data errors can introduce uncertainties in the results, with part of these errors arising from variations in CKM parameters and the remaining part originating from parameters such as form factors, decay constants, and B-meson wave functions that involve distributed amplitudes in vector meson wave functions. By employing the central values of these parameters, we initially compute numerical results for CP asymmetry and incorporate standard deviations into the error range presented in Table 2. The influence of mixed parameters on regional CP asymmetry is negligible; hence it can be disregarded without further discussion.

## V. SUMMARY AND DISCUSSION

We conducted a comprehensive analysis on the CP asymmetry in the three-body decay of B meson, focusing specifically regions on the invariant mass of  $\pi^+\pi^-$  meson pairs. The results revealed an intriguing observation - a distinct change in CP asymmetry across different resonance regions, specifically the  $\rho$ ,  $\omega$ , and  $\phi$  meson resonances. This finding suggests that these resonances play a significant role in influencing the decay dynamics and subsequent CP asymmetry. The presence of such distinct changes in CP asymmetry across different resonance regions provides valuable insights into our understanding of fundamental particle interactions. It highlights how specific energy regimes can impact particle decays and their associated symmetries.

We quantify regional CP asymmetry by integrating over the phase space. In decays such as  $\bar{B}_d \rightarrow \pi^+\pi^-\bar{K}^0$ ,  $\bar{B}_d \rightarrow \pi^+\pi^-\pi^0$ , and  $B_u^- \rightarrow \pi^+\pi^-K^-$ ,  $B_u^- \rightarrow \pi^+\pi^-\pi^-$ , we observe CP asymmetry arising from contributions of two-meson mixing and three-meson mixing processes. Notably, significant regional CP asymmetry is observed when involving  $\rho - \phi - \omega$  mixing. Experimental detection of regional CP asymmetry can be achieved by reconstructing resonant states of  $\rho$ ,  $\omega$  and  $\phi$  mesons within their respective resonance regions.

Recently, the LHCb experimental group has made significant progress in investigating the three-body decay of B meson and has obtained noteworthy findings. By analyzing previous experimental data, they have measured direct CP asymmetry in various decay modes such as  $B^\pm \rightarrow K^+K^-K^\pm$ ,  $B^\pm \rightarrow \pi^+\pi^-K^\pm$ ,  $B^\pm \rightarrow \pi^+\pi^-\pi^\pm$ , and  $B^\pm \rightarrow K^+K^-\pi^\pm$ . Building upon the achievements of LHCb experiments, future investigations are expected to

primarily focus on exploring regional CP asymmetry of the three-body decays of  $B$  meson at the resonance regions of  $\rho$ ,  $\omega$  and  $\phi$  mesons.

### Acknowledgements

This work was supported by Natural Science Foundation of Henan (Project No. 232300420115) .

- 
- [1] L. B. Okun, *Sov. Phys. Usp.* **9** (1967), 574-601.
  - [2] M. E. Shaposhnikov, *Phys. Lett. B* **277** (1992), 324-330.
  - [3] N. Cabibbo, *Phys. Rev. Lett.* **10** (1963), 531-533.
  - [4] A. Alavi-Harati *et al.* [KTeV], *Phys. Rev. Lett.* **84** (2000), 408-411.
  - [5] K. Abe *et al.* [Belle], *Phys. Rev. Lett.* **87** (2001), 091802.
  - [6] B. Aubert *et al.* [BaBar], *Phys. Rev. D* **65** (2002), 051101.
  - [7] R. Aaij *et al.* [LHCb], *Phys. Rev. Lett.* **124** (2020) no.3, 031801.
  - [8] R. Aaij *et al.* [LHCb], *Phys. Rev. D* **108** (2023) no.1, 012013.
  - [9] R. Aaij *et al.* [LHCb], *Phys. Rev. Lett.* **111** (2013), 101801.
  - [10] R. Aaij *et al.* [LHCb], *Phys. Rev. Lett.* **112** (2014) no.1, 011801.
  - [11] R. Aaij *et al.* [LHCb], *Phys. Rev. D* **90** (2014) no.11, 112004.
  - [12] X. L. Yuan, G. Lü, N. Wang, L. Y. Zhang and X. H. Guo, *Chin. Phys. C* **47** (2023) no.11, 113101.
  - [13] D. S. Shi, G. Lü, Y. L. Zhao, Na-Wang and X. H. Guo, *Eur. Phys. J. C* **83** (2023) no.4, 345.
  - [14] J. H. Christenson, J. W. Cronin, *Phys. Rev. Lett.* **13**, 138-140 (1964).
  - [15] Gang. L, Y. Lu, S.-T. Li, Y.-T. Wang, *Eur. Phys. J.* **C77**, 518 (2017).
  - [16] C. E. Wolfe, K. Maltman, *Phys. Rev.* **D80**, 114024 (2009).
  - [17] M. N. Achasov, *et.al.*, *Nucl. Phys.* **B569**, 158 (2000).
  - [18] C. E. Wolfe, K. Maltman, *Phys. Rev.* **D83**, 077301 (2011).
  - [19] L. Wolfenstein, *Phys. Rev. Lett.* **51**,1945 (1983); *Phys. Rev. Lett.* **13**, 562 (1964).
  - [20] J. J. Qi, Z. Y. Wang, X. H. Guo, X. W. Kang and Z. H. Zhang, *Nucl. Phys. B* **948** (2019), 114788.
  - [21] C. K. Chua, H. Y. Cheng and C. W. Chiang, *PoS EPS-HEP2021* (2022), 506.
  - [22] H. Y. Cheng, *Phys. Rev. D* **106** (2022) no.11, 113004
  - [23] H. Y. Cheng, C. W. Chiang and C. K. Chua, *Phys. Lett. B* **813** (2021), 136058
  - [24] R. L. Workman *et al.* (Particle Data Group). *Review of Particle Physics*, *PTEP* 2022, 083(2022).
  - [25] Y. Li, C. D. Lu, Z. J. Xiao and X. Q. Yu, *Phys. Rev. D* **70** (2004), 034009
  - [26] C. H. Chen and H. n. Li, *Phys. Lett. B* **561** (2003), 258-265
  - [27] B. Aubert *et al.* [BaBar], *Phys. Rev. D* **79** (2009), 072006.
  - [28] B. Aubert *et al.* [BaBar], *Phys. Rev. D* **78** (2008), 012004.
  - [29] A. Garmash *et al.* [Belle], *Phys. Rev. Lett.* **96** (2006), 251803.
  - [30] LHCb collaboration, R. Aaij *et al.* *Phys. Rev. Lett.* 124 (2020) 031801.